J|A|C|S
ARTICLES
Published on Web 01/26/2007

Isolation and Structural Characterization of a Family of Endohedral Fullerenes Including the Large, Chiral Cage Fullerenes $Tb_3N@C_{88}$ and $Tb_3N@C_{86}$ as well as the I_h and D_{5h} Isomers of $Tb_3N@C_{80}$

Tianming Zuo,[‡] Christine M. Beavers,[†] James C. Duchamp,[§] Anne Campbell,[‡] Harry C. Dorn,*[,‡] Marilyn M. Olmstead,[†] and Alan L. Balch*[,†]

Contribution from the Department of Chemistry, University of California, Davis, One Shields Avenue, Davis, California 95616, Department of Chemistry, Virginia Polytechnic Institute and State University, Blacksburg, Virginia 24061, and Chemistry Department, Emory and Henry College, Emory, Virginia 24327

Received September 6, 2006; E-mail: hdorn@vt.edu; albalch@ucdavis.edu

Abstract: The recent finding that isomer 2 of $Tb_3N@C_{84}$ uses one of the 51 568 possible nonisolated pentagon rule (non-IPR) structures for the C_{84} cage rather than one of the 24 cage isomers that do obey the IPR suggests that further experimental work on the structure of larger endohedrals is needed to observe the utility of the IPR rule in this uncharted territory. The structures of the newly synthesized endohedral fullerenes—$Tb_3N@C_{88}$, $Tb_3N@C_{86}$, and the I_h and D_{5h} isomers of $Tb_3N@C_{80}$— have been determined by single-crystal X-ray diffraction on samples cocrystallized with Ni^{II}(octaethylporphyrin). In contrast to the situation for isomer 2 of $Tb_3N@C_{84}$, the structures of $Tb_3N@C_{88}$ and $Tb_3N@C_{86}$ do conform to the IPR. Both $Tb_3N@C_{88}$ and $Tb_3N@C_{86}$ have chiral structures with D_2 symmetry for $Tb_3N@C_{88}$ and D_3 symmetry for $Tb_3N@C_{86}$. Within this group of endohedrals, the size of the carbon cage affects the Tb−N and Tb−C distances, the orientations of the carbon cage with respect to the porphyrin plane, the locations of the metal ions and their orientations relative to the porphyrin plane, and the degree of pyramidalization of the Tb_3N unit.

Introduction

Endohedral fullerenes, a carbon cage with an atom or atomic cluster trapped inside, have been known since the dawn of fullerene chemistry.[1,2] However, the development of the chemistry of these novel molecules has been impeded by the relatively low yields produced in the Krätschmer−Huffman arc process used for their preparation. The discovery that the inclusion of dinitrogen gas into the helium atmosphere used in the Krätschmer−Huffman generator could produce high yields of fullerenes containing the M_3N unit has made this class of endohedral fullerenes available in sufficient quantities to explore their structures, chemical reactivity, and potential utility.[3]

Considerable effort has been devoted to the examination of molecules of the type $M'_nM_{3-n}N@C_{80}$ ($n = 1\sim3$), with a carbon cage of I_h symmetry, which are formed in particularly high abundance in what has been termed the trimetallic nitride template (TNT) process. The prototypical molecule of this class, $Sc_3N@C_{80}$, is formed as one member of a family of endohedrals that includes the D_{5h} isomer of $Sc_3N@C_{80}$[4−6] along with the smaller molecules $Sc_3N@C_{78}$[7] and $Sc_3N@C_{68}$.[8,9] When larger metal ions are employed in the TNT process, families of endohedrals are produced that include carbon cages larger than C_{80} but in significantly lower abundance. For example, Yang and Dunch have reported the formation of a family of dysprosium endohedrals that includes two isomers of $Dy_3N@C_{78}$, three isomers of $Dy_3N@C_{80}$, $Dy_3N@C_{82}$, two isomers of $Dy_3N@C_{84}$, $Dy_3N@C_{86}$, $Dy_3N@C_{88}$, $Dy_3N@C_{90}$, $Dy_3N@C_{92}$, $Dy_3N@C_{94}$, $Dy_3N@C_{96}$, and $Dy_3N@C_{98}$.[10,11] Similarly, Krause, Wong, and Dunsch found that thulium produced a somewhat less extensive set of endohedral fullerenes including $Tm_3N@C_{78}$, two isomers of $Tm_3N@C_{80}$, $Tm_3N@C_{82}$, two isomers of $Tm_3N@C_{84}$, and $Tm_3N@C_{86}$.[12] However, definitive structural

[†] University of California.
[‡] Virginia Polytechnic Institute and State University.
[§] Emory and Henry College.

(1) Heath, J. R.; O'Brien, S. C.; Zhang, Q.; Liu, Y.; Curl, R. F.; Kroto, H. W.; Tittel, F. K.; Smalley, R. E. *J. Am. Chem. Soc.* **1985**, *107*, 7779.
(2) Akasaka, T., Nagase, S. Eds. *Endofullerenes: A New Family of Carbon Clusters*; Kluwer Academic Publishers: Dordrecht, The Netherlands, 2002.
(3) Stevenson, S.; Rice, G.; Glass, T.; Harich, K.; Cromer, F.; Jordan, M. R.; Craft, J.; Hadju, E.; Bible, R.; Olmstead, M. M.; Maitra, K.; Fisher, A. J.; Balch, A. L.; Dorn, H. C. *Nature* **1999**, *401*, 55.
(4) Duchamp, J. C.; Demortier, A.; Fletcher, K. R.; Dorn, D.; Iezzi, E. B.; Glass. T.; Dorn, H. C. *Chem. Phys. Lett.* **2003**, *375*, 655−659.
(5) Krause, M.; Dunsch, L. *ChemPhysChem* **2004**, *5*, 1445.
(6) Cai, T.; Xu, L.; Anderson, M. R.; Ge, Z.; Zuo, T.; Wang, X.; Olmstead, M. M.; Balch, A. L.; Gibson, H. W.; Dorn, H. C. *J. Am. Chem. Soc.* **2006**, *128*, 8581.
(7) Olmstead, M. M.; de Bettencourt-Dias, A.; Duchamp, J. C.; Stevenson, S.; Marciu, D.; Dorn, H. C.; Balch, A. L. *Angew. Chem., Int. Ed.* **2001**, *40*, 1223.
(8) Stevenson, S.; Fowler, P. W.; Heine, T.; Duchamp, J. C.; Rice, G.; Glass, T.; Harich, K.; Hajdu, E.; Bible, R.; Dorn, H. C. *Nature* **2000**, *408*, 427.
(9) Olmstead, M. M.; Lee, H. M.; Duchamp, J. C.; Stevenson, S.; Marciu, D.; Dorn, H. C.; Balch, A. L. *Angew. Chem., Int. Ed.* **2003**, *42*, 900.
(10) Yang, S.; Dunsch, L. *J. Phys. Chem. B* **2005**, *109*, 12320.
(11) Yang, S.; Dunsch, L. *Chem.−Eur. J.* **2006**, *12*, 413.

characterization of most of the members of these families of larger endohedral fullerenes is lacking.

As the size of the fullerene cage increases, the possibilities for the existence of multiple isomers also increases. Most fullerenes and endohedral fullerenes obey the isolated pentagon rule (IPR), which requires that each of the twelve pentagons in the carbon cage be surrounded by hexagons. Thus, for C_{80} there are 9 isomeric structures that conform to the IPR, but for C_{88} there are 35 IPR structures and for C_{86} there are 19 IPR structures.[13] In the families of large fullerenes that can form with larger lanthanide ions inside, will only a few selected isomeric structures be formed or will complex mixtures of many isomers be found that produce new challenges in their separation? To compound the issue of structural variety, endohedral fullerenes exist that violate the IPR. No IPR structures exist for cages containing 62, 64, 66, or 68 carbon atoms. Nevertheless, a non-IPR structure for $Sc_3N@C_{68}$[8] was first reported utilizing NMR and computational studies, and the structure subsequently was confirmed by a single-crystal X-ray diffraction study.[9] It has also been reported that $Sc_2@C_{66}$[14] and $Sc_2C_2@C_{68}$[15] adopt non-IPR structures on the basis of MEM powder X-ray diffraction and NMR studies, respectively. In each, the metals are contained within the pentalene units formed where pairs of pentagons abut.

Recently, we have reported that two isomers of $Tb_3N@C_{84}$ could be isolated using the TNT process with Tb_4O_7-doped graphite rods.[16] The structure of isomer 2, the more abundant isomer, has been determined by single-crystal X-ray diffraction. Remarkably, the structure does not obey the IPR. There are 24 IPR isomeric structures available for a C_{84} cage, but isomer 2 of $Tb_3N@C_{84}$ adopts a non-IPR structure with C_s symmetry and a single site where two pentagonal rings abut. For a C_{84} cage, there are 51 568 isomeric structures that do not conform to the IPR but have cages composed of only pentagons and hexagons.[13] The finding that isomer 2 of $Tb_3N@C_{84}$ uses one of these 51 568 non-IPR structures suggests that the structures of larger endohedral fullerenes will be difficult to predict, since one can no longer anticipate a priori that the IPR will pertain and limit the isomers that can form (see Note Added in Proof). Clearly, single-crystal X-ray diffraction studies on these larger endohedrals are needed in order to ascertain their structures.

Results

Preparation and Isolation of the $Tb_3N@C_{2n}$ ($n = 40-44$) Family of Endohedrals. Raw soot containing the $Tb_3N@C_{2n}$ ($n = 40-44$) family of endohedrals was synthesized in an arc-discharge generator by vaporizing composite graphite rods containing a mixture of Tb_4O_7, graphite powder, and iron nitride (Fe_xN) with a weight ratio of 2.03:1.0:0.4, respectively. From previous studies, it has been established that the presence of Fe_xN enhances the yield of trimetallic nitride endohedral metallofullerenes. Together with the graphite tube for packing the above mixture, the molar ratio of Tb:C is about 4%. The arc-discharge process was conducted in a dynamic flow of helium and about 3% dinitrogen. The pressure was about 300 Torr at the start of the arc-discharge. The raw soot was extracted using toluene as a solvent in a Soxhlet extractor for 20 h. The HPLC chromatogram of the extract is shown in Figure 1a.

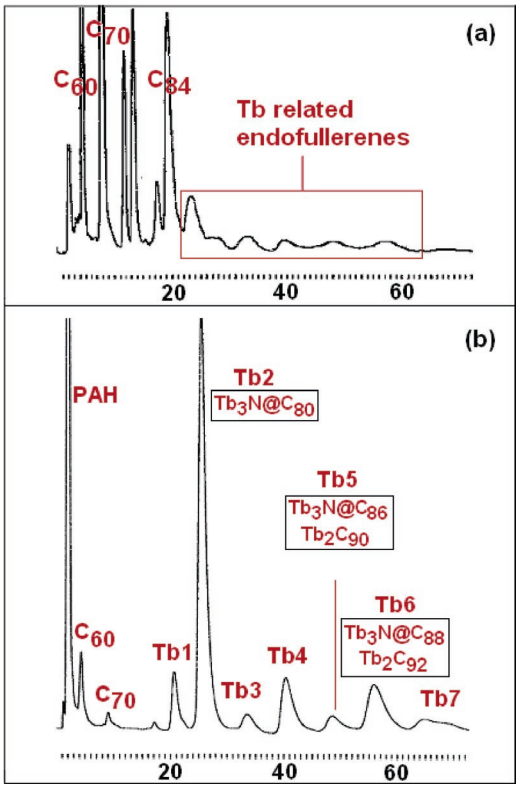

Figure 1. (a) HPLC chromatogram of the toluene extract from the arc-discharge with Tb_4O_7. (b) HPLC chromatogram on a 5PBB column (4.6 mm × 250 mm with $\lambda = 390$ nm detection; 2.0 mL/min of toluene) of the eluent from the CPDE-MPR column.

The primary purification process was carried out using a chemical separation method. The toluene extract was subject to chemical separation on a cyclopentadiene functionalized Merrifield peptide resin (CPDE-MPR) column.[17] The HPLC chromatogram for the recovered sample after the chemical separation utilizing the CPDE-MPR column is shown in Figure 1b. This approach relies on the inherent chemical kinetic stability of trimetallic nitride endohedral metallofullerenes (TNT EMFs) relative to empty-cage fullerenes and non-TNT EMFs. Since the TNT EMFs, $A_3N@C_{2n}$ ($78 \leq 2n \leq 88$), are all large-gap compounds (HOMO−LUMO gap >1.0 eV),[18−20] they are all relatively kinetically stable species (although their individual kinetic stabilities may differ). By comparison of Figure 1 parts a and b, we know that the chemical separation process also concentrated the TNT EMFs by getting rid of most of the reactive fullerenes. If the CPDE-MPR column approaches saturation, peaks due to C_{60} and C_{70} appear in the subsequent chromatogram of the eluent as shown in Figure 1b. The larger cage TNT EMFs ($2n > 80$) also pass through the CPDE-MPR column and were eluted. In Figure 1b, there are seven fractions that are labeled Tb1 to Tb7. Although the analysis of each

(12) Krause, M.; Wong, J.; Dunsch, L. *Chem.−Eur. J.* **2005**, *11*, 706.
(13) Fowler, P. W.; Manolopoulos, D. E. *An Atlas of Fullerenes*; Clarendon Press: Oxford, 1995.
(14) Wang, C.-R.; Kai, T.; Tomiyama, T.; Yoshida, T.; Kobayashi, Y.; Nishibori, E.; Takata, M.; Sakata, M.; Shinohara, H. *Nature* **2000**, *408*, 426.
(15) Shi, Z.; Wu, X.; Wang, C.-R.; Lu, X.; Shinohara, H. *Angew. Chem., Int. Ed.* **2006**, *45*, 2107.
(16) Beavers, C. M.; Zuo, T.; Duchamp, J. C.; Harich, K.; Dorn, H. C.; Olmstead, M. M.; Balch, A. L. *J. Am. Chem. Soc.* **2006**; *128*, 11352.
(17) Ge, Z.; Duchamps, J. C.; Cai, T.; Gibson, H. W.; Dorn, H. C. *J. Am. Chem. Soc.* **2005**, *127*, 16292.
(18) Krause, M.; Dunsch, L. *Angew. Chem., Int. Ed.* **2005**, *44*, 1557.
(19) Krause, M.; Wong, J.; Dunsch, L. *Chem.−Eur. J.* **2005**, *11*, 706.
(20) Yang, S.-F.; Dunsch, L. *J. Phys. Chem. B* **2005**, *109*, 12320.

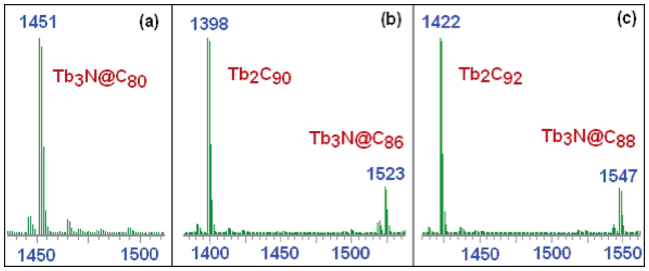

Figure 2. Negative ion DCI MS spectra of (a) fraction Tb2, (b) fraction Tb4, and (c) fraction Tb6 from the chromatogram in Figure 1b.

fraction has not been completed, the tentative identities of the components in each fraction are indicated in Figure 1b. For example, fraction Tb2 contains $Tb_3N@C_{80}$ (I_h and D_{5h} isomers); fraction Tb5 contains $Tb_3N@C_{86}$ and Tb_2C_{90}; and fraction Tb6 contains $Tb_3N@C_{88}$ and Tb_2C_{92}. The mass spectra of material present in fractions Tb2, Tb5, and Tb6 are shown in Figure 2.

The fractions labeled Tb2, Tb5, and Tb6 were purified further using a 5PYE column. In this fashion, pure samples of the I_h and D_{5h} isomers of $Tb_3N@C_{80}$, $Tb_3N@C_{86}$, and $Tb_3N@C_{88}$ were obtained. The HPLC chromatograms, UV−vis, and MS spectra of the purified samples are shown in the Supporting Information as Figures SI-1, SI-2, and SI-3, respectively.

Structural Studies. Each of these new endohedrals has been crystallized in the presence of Ni^{II}(OEP) (OEP is the dianion of octaethylporphyrin) to produce samples suitable for single-crystal X-ray diffraction studies. Table 1 contains comparative interatomic distance and angle information for the Tb_3N units inside the cages. Crystal data are contained in Table 2. The endohedrals crystallize with the stoichiometry of one molecule of the fullerene, one molecule of Ni^{II}(OEP) and two molecules of benzene, except in the cases of $Tb_3N@C_{88}$ where there are two and a half molecules of benzene present and $Tb_3N@C_{86}$ which has three molecules of benzene. Figures 3, 4, 5, and 6 are drawings that show each endohedral and its spatial relationship to the porphyrin. In every case the porphyrin portion adopts a nearly planar structure like that observed in the triclinic form of Ni^{II}(OEP)[21] rather than the S_4 distorted structure found in the tetragonal polymorph of pristine Ni^{II}(OEP).[22] Notice that the orientations of the Tb_3N groups inside the cages vary from one compound to another. Each of the structures displays some degree of disorder (vide infra), and only the major orientation of the fullerene and its contents is shown in Figures 3−6.

The Structure of $Tb_3N@C_{88}$. Figure 3 shows the relationship between the endohedral and the porphyrin, while Figure 7 shows a stereoscopic drawing of the carbon skeleton of the cage. The carbon cage itself has an IPR structure with D_2 symmetry. The thirty-five possible IPR isomers for a cage of 88 carbons have the following symmetries: C_1, 11 different isomers; C_s, 11 isomers; C_2, 7 isomers; C_{2v}, 3 isomers; D_2, 2 isomers; and T_d, 1 isomer. The isomer found in $Tb_3N@C_{88}$ is number 35 in the list of Fowler and Manopolous.[13] The C_{88} cage is the largest fullerene to date to have its structure determined crystallographically. As the stereoview in Figure 7 shows, the carbon cage of $Tb_3N@C_{88}$ has a rather flattened shape. This flattening is indicated by the rather short C···C distance (7.245 Å) along one of the C_2 axes and longer distances (8.839 and 8.531 Å) along the other two C_2 axes.

Table 1. Selected Interatomic Distances and Angles

	$Tb_3N@C_{88}$·Ni^{II}(OEP)·2.5C6H6	$Tb_3N@C_{88}$·Ni^{II}(OEP)·2.5C_6H_6	$Tb_3N@C_{86}$·Ni^{II}(OEP)·3C_6H_6	$Tb_3N@C_{86}$·Ni^{II}(OEP)·3C_6H_6
site	site 1	site 2	site 1	site 2
occupancy	0.43	0.40	0.60(2)	0.40(2)
distances (Å)				
Tb1−N1	2.207(3)	2.175(3)	2.158(6)	2.165(7)
Tb2−N1	2.171(3)	2.209(3)	2.159(3)	2.148(7)
Tb3−N1	2.180(3)	2.175(3)	2.159(3)	2.151(7)
Tb1-C	2.333(10)	2.418(8)	2.454(13)	2.36(2)
Tb2-C	2.430(9)	2.337(10)	2.398(19)	2.383(19)
Tb3-C	2.328(8)	2.382(9)	2.398(19)	2.373(17)
angles (deg)				
Tb1−N1−Tb2	117.26(12)	116.46(13)	119.53(14)	119.1(3)
Tb1−N1−Tb3	117.40(13)	125.22(14)	119.53(14)	118.8(3)
Tb2−N1−Tb3	125.23(13)	118.23(13)	120.3(3)	121.7(3)
∑(Tb−N−Tb)	359.89	359.91	359.36	359.6
	D_{5h} isomer of $Tb_3N@C_{80}$·Ni^{II}(OEP)·2C_6H_6	I_h isomer of $Tb_3N@C_{80}$·Ni^{II}(OEP)·2C_6H_6	I_h isomer of $Tb_3N@C_{80}$·Ni^{II}(OEP)·2C_6H_6	isomer 2 of $Tb_3N@C_{84}$·Ni^{II}(OEP)·2C_6H_6[a]
site	site 1	site 1, N1A	site 2, N1B	site 1
occupancy	0.341(2)	0.60	0.40	0.512(3)
distances (Å)				
Tb1−N1	2.008(8)	2.056(4)	2.038(6)	2.182(4)[b]
Tb2−N1	2.026(6)	2.089(4)	2.085(6)	2.130(4)
Tb3−N1	2.130(6)	2.077(4)	2.089(4)	2.120(4)
Tb1-C	2.287(17)	2.423(3)		2.483(6)
Tb2-C	2.315(15)	2.434(3)		2.406(6)
Tb3-C	2.18(2)	2.404(3)		2.333(6)
angles (deg)				
Tb1−N1−Tb2	125.0(3)	116.78(18)	117.8(3)	124.5(2)
Tb1−N1−Tb3	110.8(3)	117.65(19)	118.8(3)	114.6(2)
Tb2−N1−Tb3	111.9(4)	111.63(18)	112.1(3)	120.7(2)
∑(Tb−N−Tb)	347.7	346.06	348.7	359.8

[a] Data from ref 16. [b] This distance is long because of the position of Tb1 in the nose of the elongated portion of the fullerene.

The cage is disordered with the two enantiomers residing at a common site. Although there is only one nitrogen atom site inside the cage, the positions of the terbium atoms are also disordered. There are two major sets of three Tb atoms. One involves Tb1, Tb2, and Tb3 and has 0.43 fractional occupancy. This is the set shown in Figure 3. The other involves Tb4, Tb5, and Tb6 with 0.40 fractional occupancy. Additionally, there are four minor sets of three Tb positions with 0.07, 0.04, 0.03, and 0.03 occupancies.

The Tb_3N units are planar in each orientation. The sum of the Tb−N−Tb angles for the major site is 359.89°. Similarly, for the site involving Tb4, Tb5, and Tb6, the sum of the three Tb−N−Tb angles is 359.91°. At the major sites the Tb−N distances fall in a narrow range: 2.171(3)−2.207(3) Å for the site with 0.43 occupancy and 2.175(3)−2.209(3) at the site with 0.40 occupancy. Complete specification of the orientation of the Tb_3N unit with respect to the carbon cage is not possible, since there are two cage orientations that combine with two major and four minor Tb_3N locations.

$Tb_3N@C_{86}$. Like $Tb_3N@C_{88}$, $Tb_3N@C_{86}$ has a flattened cage that is chiral. Figure 4 shows a drawing of the endohedral and its relationship to the porphyrin in the crystal. The fullerene is oriented with its flat side facing the porphyrin. Figure 8 shows a stereoscopic drawing of the cage itself, which has D_3 symmetry. This cage does obey the IPR and is number 17 on the list of 17 IPR isomers computed by Fowler and Manopolous for C_{86}.[13]

(21) Brennan, T. D.; Scheidt, W. R.; Shelnutt, J. A. *J. Am. Chem. Soc.* **1988**, *110*, 3919.
(22) Meyer, E. F., Jr. *Acta Crystallogr., Sect. B* **1972**, *28*, 2162.

Table 2. Crystallographic Data

	$Tb_3N@C_{88}$·Ni^{II}(OEP)·$2.5C_6H_6$	$Tb_3N@C_{86}$·Ni^{II}(OEP)·$3C_6H_6$	I_h isomer of $Tb_3N@C_{80}$·Ni^{II}(OEP)·$2C_6H_6$	D_{5h} isomer of $Tb_3N@C_{80}$·Ni^{II}(OEP)·$2C_6H_6$
color/habit	black parallelepiped	black parallelepiped	black parallelepiped	black parallelepiped
formula	$C_{139}H_{59}N_5NiTb_3$	$C_{134}H_{56}N_5NiTb_3$	$C_{128}H_{56}N_5NiTb_3$	$C_{128}H_{56}N_5NiTb_3$
fw	2334.38	2271.31	2199.25	2199.25
cryst syst	triclinic	monoclinic	monoclinic	monoclinic
space group	$P\bar{1}$	$C2/m$	$C2/c$	$C2/m$
a, Å	14.990(3)	25.2024(8)	25.3036(8)	25.2505(7)
b, Å	16.795(3)	15.4733(5)	15.0584(5)	15.1262(4)
c, Å	18.408(3)	19.9878(7)	39.3947(13)	19.7335(5)
α, deg	77.940(3)	90	90	90
β, deg	76.268(3)	92.5450(10)	95.2030(10)	95.438(3)
γ, deg	65.161(3)	90	90	90
V, Å^3	4053.9(13)	7786.8(4)	14948.8(9)	7503.2(3)
Z	2	4	8	4
T, K	90(2)	90(2)	90(2)	90(2)
λ, Å	0.71073	0.71073	0.71073	0.71073
ρ, g/cm^3	1.912	1.937	1.954	1.947
μ, mm^{-1}	2.886	3.002	3.124	3.112
R1 (obsd data)[a]	0.056	0.054	0.035	0.079
wR2 (all data)[b]	0.122	0.141	0.083	0.234

[a] For data with $I > 2\sigma I$: $R1 = \sum||F_o| - |F_c||/\sum|F_o|$. [b] For all data: $wR2 = [\sum[w(F_o^2 - F_c^2)^2]/\sum[w(F_o^2)^2]]^{1/2}$.

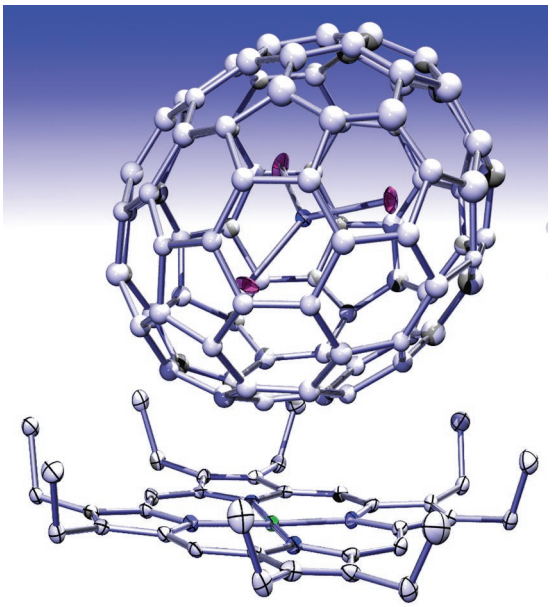

Figure 3. A perspective view of the fullerene and Ni^{II}(OEP) molecules in $Tb_3N@C_{88}$·Ni(OEP)·$2.5C_6H_6$ showing 50% thermal contours. Only one position of the carbon cage and the major Tb_3N site are shown.

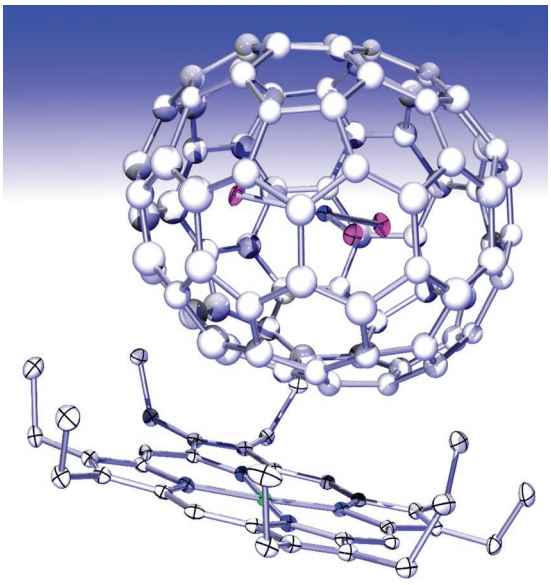

Figure 4. A perspective view of the fullerene and Ni^{II}(OEP) molecules in $Tb_3N@C_{86}$·Ni(OEP)·$2C_6H_6$ showing 50% thermal contours. Only one position of the carbon cage and the major Tb_3N site are shown.

The dimensions of the cage give a measure of its flattened nature. The surface-to-surface distance along the cage's 3-fold axis is 7.353 Å, while along the three 2-fold axes that are perpendicular to the principal axis, the corresponding distances are 8.516, 8.555, and 8.553 Å.

The asymmetric unit consists of two quarter-molecules of the fullerene, one-half of the nickel porphyrin, and one and one-half molecules of benzene. The nickel porphyrin resides on a mirror plane that bisects N2, Ni, and N4. One of the benzene molecules resides in a general position while the other resides on a mirror plane. These units are all ordered. However, there is disorder in the positioning of the endohedral. A complete C_{86} cage is generated by combining one of the quarter C_{86} units with the mirror image of the other quarter C_{86} unit to produce a chiral fullerene with 0.50 fractional occupancy. A second cage at 0.50 fractional occupancy is produced by combining the mirror image of the first quarter C_{86} unit with the other quarter C_{86} unit. Inside the cage, there is one nitrogen atom site, which is located on a mirror plane, and several sites for the terbium atoms. The principle site for the Tb_3 unit has 0.60(2) occupancy and involves Tb1, which is situated on a mirror plane, and Tb2, which sits in a general position. Tb3, Tb4, and Tb5, which all reside in general positions, provide a second site that has 0.40(2) total occupancy when it and its mirror image produced by reflection are considered.

In each Tb_3 site the Tb_3N unit is planar. For the major site the sum of the Tb−N−Tb angles is 359.36°. Similarly, the sum of the three Tb−N−Tb angles is 359.60° for the minor site. The Tb−N distances in the major site are 2.158(6) and 2.159(3) Å. At the minor site the Tb−N distances are similar, 2.165-

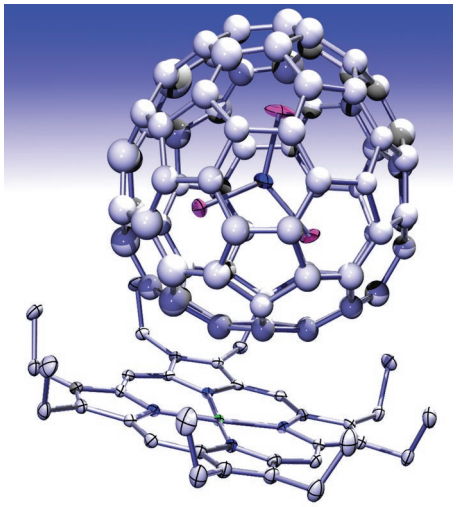

Figure 5. A perspective view of the fullerene and $Ni^{II}(OEP)$ molecules in the D_{5h} isomer of $Tb_3N@C_{80}\cdot Ni(OEP)\cdot 2C_6H_6$ showing 50% thermal contours. Only one position of the carbon cage and the major Tb_3N site are shown.

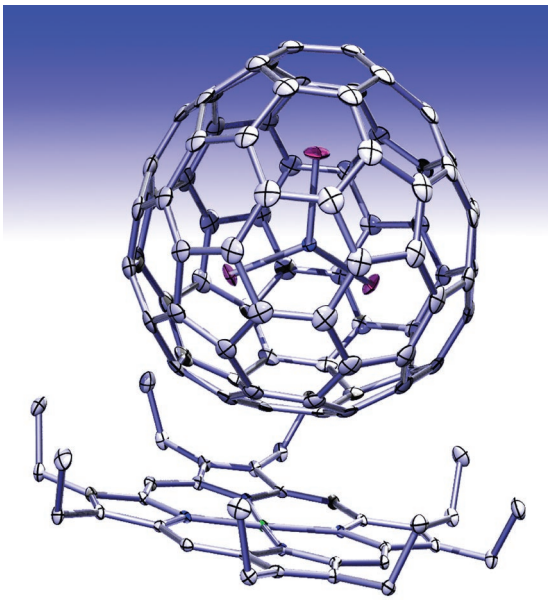

Figure 6. A perspective view of the fullerene and $Ni^{II}(OEP)$ molecules in the I_h isomer of $Tb_3N@C_{80}\cdot Ni(OEP)\cdot 2C_6H_6$ showing 50% thermal contours. Only one position of the carbon cage and the major Tb_3N site are shown.

(7), 2.148(7), and 2.151(7) Å. Notice that the Tb−N distances in $Tb_3N@C_{86}$ are all shorter than the Tb−N distances found in $Tb_3N@C_{88}$.

Figure 9 shows the location of the major Tb_3N site within the C_{86} cage. The Tb_3N unit is positioned to coincide with the 3-fold symmetry of the D_3 symmetry of the carbon cage with the nitrogen atom located midway between C1 and C86. Figure 10 shows the locations of the nearest carbon atoms in the C_{86} cage and the terbium ions for the major site. Each terbium ion is situated over a pair of carbon atoms at a 6:6 ring junction.

The (D_{5h}) Isomer of $Tb_3N@C_{80}$. The structure of the fullerene cage in the D_{5h} isomer of $Tb_3N@C_{80}$ is similar to that previously reported for the D_{5h} isomer $Sc_3N@C_{80}$. Figure 5 shows a drawing of the structure and its relationship to the adjacent porphyrin. The asymmetric unit of the $(D_{5h})Tb_3N@C_{80}\cdot Ni^{II}(OEP)\cdot 2C_6H_6$ consists of the fullerene cage at half occupancy, one-half of the nickel porphyrin, two half molecules of benzene, one-half of the nitrogen atom, and various disordered terbium atoms. The nickel porphyrin resides on a mirror plane that bisects N2, Ni, and N4. One of the benzene molecules resides on a horizontal mirror plane in a general position, while the other resides on a vertical mirror plane. The fullerene and its contents are disordered. The fullerene packs around a mirror plane that does not coincide with a mirror plane of the D_{5h} structure. Consequently, the entire cage was located and refined at 0.50 occupancy for all carbon sites. The crystallographic mirror symmetry produces a second cage that occupies the same site with a second orientation.

The terbium atoms are distributed over twelve individual positions that can be divided into four sites based in part upon their populations. Site 1 (Tb1, Tb2, Tb3) is the predominant site and has refined fractional occupancy of 0.682(2). Site 2 (Tb4, Tb5, Tb6) has the lowest occupancy, 0.070(1). Sites 3 (Tb7, Tb8, Tb9) and 4 (Tb10, Tb11, Tb12) have the same occupancy, 0.124(2), and are distinguished by the angular disposition of the individual terbium atoms. *The Tb_3N portions are pyramidal in each of these four sites.* The sum of the three Tb−N−Tb angles at the individual sites are 347.8° for site 1, 358.9° for site 2, 350.8° for site 3, and 349.5° for site 4.

Figure 11 shows the relationships between the central Tb_3N group and the cage that surrounds it. The Tb_3N unit is oriented so that the plane of the Tb_3 atoms makes an angle of 68° with the horizontal mirror plane that runs perpendicular to the 5-fold axis of the fullerene. This contrasts with the situation in D_{5h}-$Sc_3N@C_{80}$ where the Sc_3N group is planar and this group is tipped by 30° from the horizontal mirror plane. The closest contacts between the terbium ions and the cage carbon atoms involve the interactions with pairs of carbon atoms located at 6:6 ring junctions that are positioned between a hexagon and a pentagon.

The (I_h) Isomer of $Tb_3N@C_{80}$. Crystals of $(I_h)Tb_3N@C_{80}\cdot Ni^{II}(OEP)\cdot 2C_6H_6$ show much less disorder than any of the other three compounds considered here. Figure 6 shows a drawing of the overall structure, while Figure 12 shows the relationship between the Tb_3N group and the carbon cage.

The asymmetric unit consists of the endohedral, a molecule of nickel porphyrin, and two molecules of benzene, all in general positions. The geometry of the carbon cage shows the expected idealized I_h symmetry. Inside the cage, the predominant terbium ions sites have 0.97 occupancy. There are two sites for the nitrogen atoms with occupancy of 0.60 for N1A and 0.40 for N1B. Thus, there are two prevalent sites for the Tb_3N unit. In each position the Tb_3N unit is *pyramidalized*. The sum of the three Tb−N−Tb angles is 346.06° for the site involving N1A and 348.7° for the site involving N1B.

As the data in Table 1 show, the Tb−N distances in (I_h)-$Tb_3N@C_{80}$ are shorter than those in $Tb_3N@C_{88}$ and $Tb_3N@C_{86}$ but are similar to those seen in $(D_{5h})Tb_3N@C_{80}$. The Tb−C distances are also similar to those found in $(D_{5h})Tb_3N@C_{80}$ and longer than those in the two larger endohedrals.

Figure 12 shows the location of the Tb_3N unit with regard to the carbon atoms of the cage. It is noteworthy that the metal atoms are located near the centers of hexagons on the fullerene. For comparison, in the Diels−Alder cycloadduct $Sc_3N@C_{80}$−$C_{10}H_{12}O_2$, which displays a similar degree of order in regard to

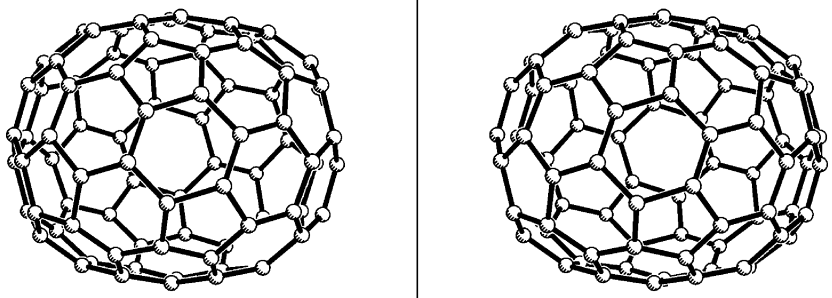

Figure 7. A stereoscopic drawing of one enantiomer of the C_{88} carbon cage in $Tb_3N@C_{88}\cdot Ni^{II}(OEP)\cdot 2.5C_6H_6$. One of the 2-fold axes is aligned vertically. The distance along the vertical C_2 axis (from the center of the C1−C2 bond to the center of the C87−C88 bond) is 7.245 Å. In contrast, the distances along the other two C_2 axes are greater; 8.839 Å for the distance from the center of the C43−C44 bond to the center of the C55−C56 bond and 8.531 Å from the center of the hexagon containing C26 and C27 and the center of the hexagon containing C37 and C38.

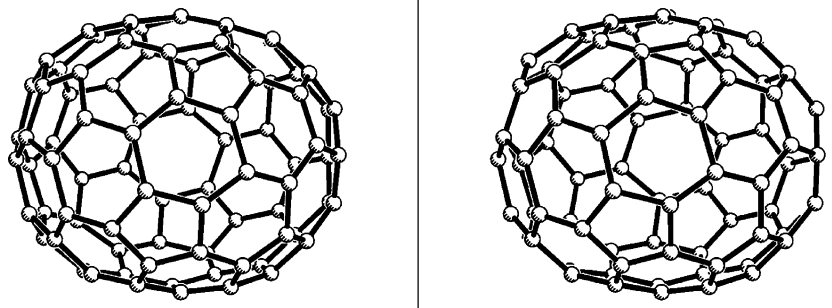

Figure 8. A stereoscopic drawing of one enantiomer of the C_{86} carbon cage in $Tb_3N@C_{86}\cdot Ni^{II}(OEP)\cdot 3C_6H_6$. The C_3 axis is aligned vertically. The distance along the C_3 axis between C1 and C82 is 7.353 Å. In contrast, the distances from one side of the cage to the other along the three 2-fold axes (8.516, 8.555, and 8.552 Å) average 8.541 Å.

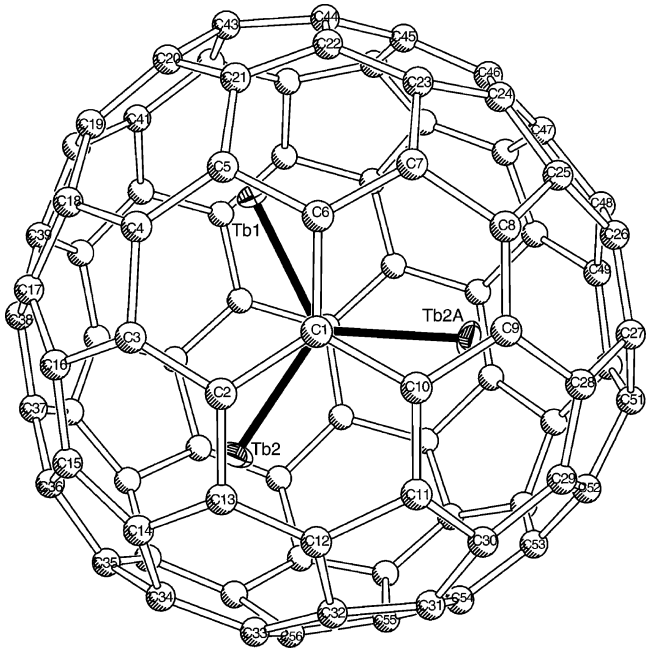

Figure 9. A view down the 3-fold axis of $Tb_3N@C_{86}$ showing the location of the major (0.60 occupancy) site for the Tb_3N group inside the cage.

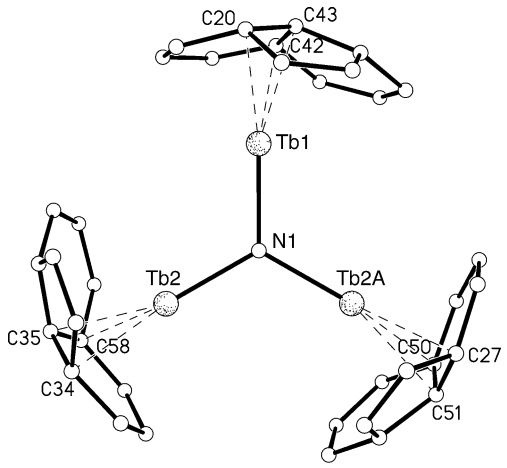

Figure 10. A drawing of $Tb_3N@C_{86}$ showing the interactions between the major site for the terbium ions and the closest carbon atoms within the cage.

the Sc_3N unit and the carbon cage, the scandium ions are located near pairs of carbon atoms, not over hexagons.[23] A comparison with the structure of unfunctionalized $(I_h)Sc_3N@C_{80}$ would be more appropriate, but the available data are limited to disordered structures where there are multiple metal sites to consider.

In order to see the effects of metal atom placement on the structure of the carbon cages in endohedrals, it is useful to examine the pyramidalization angles, θ_p,[24] (θ_p for graphite = 0°; θ_p for C_{60} = 11.6°), for the individual fullerene carbons of

(23) Lee, H. M.; Olmstead, M. M.; Iezzi, E.; Duchamp, J. C.; Dorn, H. C.; Balch, A. L. *J. Am. Chem. Soc.* **2002**, *124*, 3494.

(24) Haddon, R. C.; Raghavachari, K. In *Buckminsterfullerenes*; Billups, W. E., Ciufolini, M. A., Eds.; VCH: New York, 1993; Chapter 7.

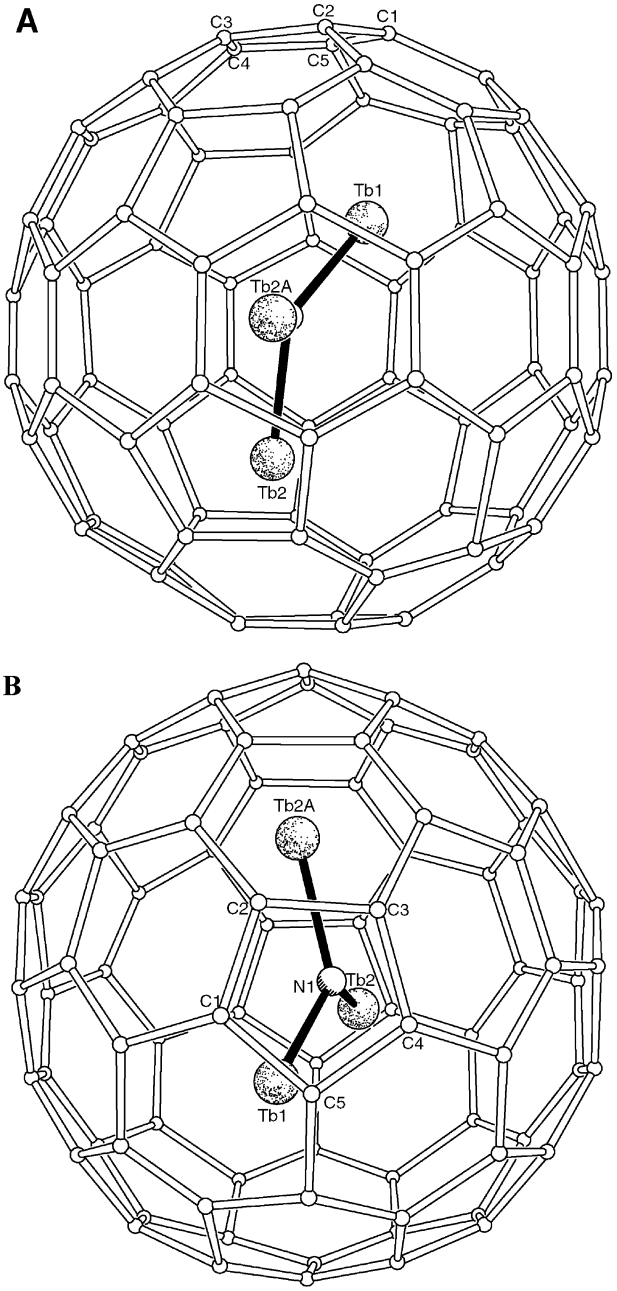

Figure 11. Two orthogonal views of $(D_{5h})Tb_3N@C_{80}$ in $(D_{5h})Tb_3N@C_{80}$·Ni(OEP)·$2C_6H_6$ showing the location of the major site of Tb_3N unit within the carbon cage. In graphic A the 5-fold axis of the carbon cage is vertical, while in graphic B the view is directed down the 5-fold axis.

the cage. Figure 13 shows a plot of θ_p for the carbon atoms in $(I_h)Tb_3N@C_{80}$. Within an isocahedral C_{80} cage there are two types of carbon atoms, those at the intersection of three hexagons (3hC) and those at the intersection of two hexagons and a pentagon (2hC). As seen in Figure 13 the 2hC carbons atoms generally are more pyramidalized than the 3hC carbon atoms when those carbon atoms lying closest to the terbium ions are omitted from consideration. The 3hC carbon atoms have pyramidalizations that fall in a rather narrow range, 8.41−9.13°, the pyramidalizations of the 2hC atoms span a larger range, 8.42−10.86°. However, the 18 carbon atoms that lie over the terbium ions are the most pyramidalized. Within this group, the atoms in the 2hC class show larger pyramidalizations that fall in the range 11.32−13.00°, which is larger than those of

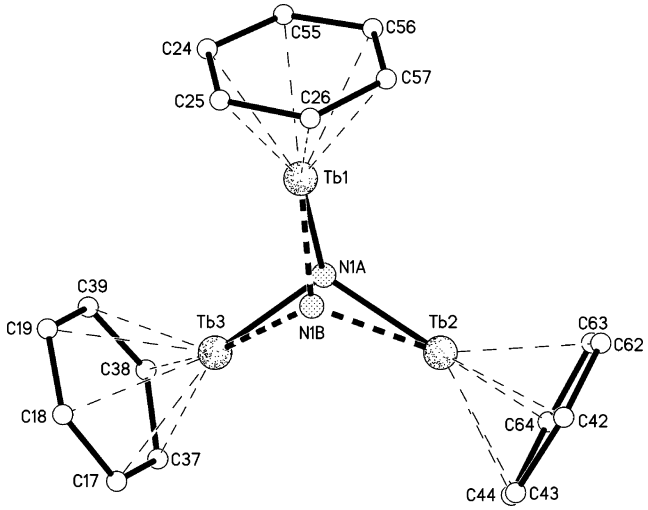

Figure 12. The location of the Tb atoms with regard to the two positions for the nitrogen atom and carbon atoms of the cage in $(I_h)Tb_3N@C_{80}$·Ni^{II}-(OEP)·$2C_6H_6$.

the type 3hC, which fall in the range 10.59−11.59°. Similar effects of metal atoms producing greater pyramidalization for neighboring carbon atoms have been observed in other endohedrals, $(D_{5h})Sc_3N@C_{80}$[6] and $(I_h)CeSc_2@C_{80}$,[25] and in some functionalized endohedrals that crystallize with sufficient order to make it possible to determine the pyramidalizations.[26] It is interesting to note that larger pyramidalizations (ca 14.0°) are found in the Diels−Alder cycloadduct, $Sc_3N@C_{80}-C_{10}H_{12}O_2$,[23] despite the fact that the ionic radius of scandium is less than that of terbium. However, in that case the scandium ions reside close to pairs of carbons atoms, which are the carbon atoms showing the high degree of pyramidalization, whereas in (I_h)-$Tb_3N@C_{80}$, the terbium atoms sit over hexagons and push the adjacent six carbon atoms away from the fullerene surface.

The carbon−carbon bond distances in $(I_h)Tb_3N@C_{80}$ also show the effects of the proximity of interior metal atoms. If those bonds closest to the terbium ions are omitted, the average C−C bond length at the 6:5 ring junctions (1.440(1) Å) is slightly longer than the average C−C bond length at the 6:6 ring junctions (1.427(1) Å). A similar situation pertains in the Diels−Alder cycloadduct, $Sc_3N@C_{80}-C_{10}H_{12}O_2$, where the average 6:5 C−C bond distance, (excluding those in the vicinity of the addend) is 1.437(15) Å, while average 6:6 C−C bond distances is 1.421(18) Å. Note that in C_{60} the average 6:5 and 6:6 bond distances (1.453(5) and 1.383(4) Å, respectively) differ by a larger amount.[27] In $(I_h)Tb_3N@C_{80}$ the terbium atoms lengthen the adjacent C−C bonds. For the 18 carbon atoms closest to terbium ions, the average C−C bond length at the 6:5 ring junctions (1.477(1) Å) and the average C−C bond length at the 6:6 ring junctions (1.458(1) Å) are longer than the average bond lengths for the carbon atoms further from the terbium atoms.

Discussion

Five members of the $Tb_3N@C_{2n}$ family of endohedrals have been crystallographically characterized, which makes this the

(25) Wang, X.; Zuo, T.; Olmstead, M. M.; Duchamp, J. C.; Glass, T. E.; Cromer, T. E.; Balch, A. L.; Dorn, H. C. *J. Am. Chem. Soc.* **2006**, *128*, 8884.
(26) Echegoyen, L.; Chancellor, C. J.; Cardona, C. M.; Elliot, B.; Rivera, J.; Olmstead, M. M.; Balch, A. L. *Chem. Commun*. **2006**, 2653.
(27) Fedurco, M.; Olmstead, M. M.; Fawcett, W. R. *Inorg. Chem.* **1995**, *34*, 390.

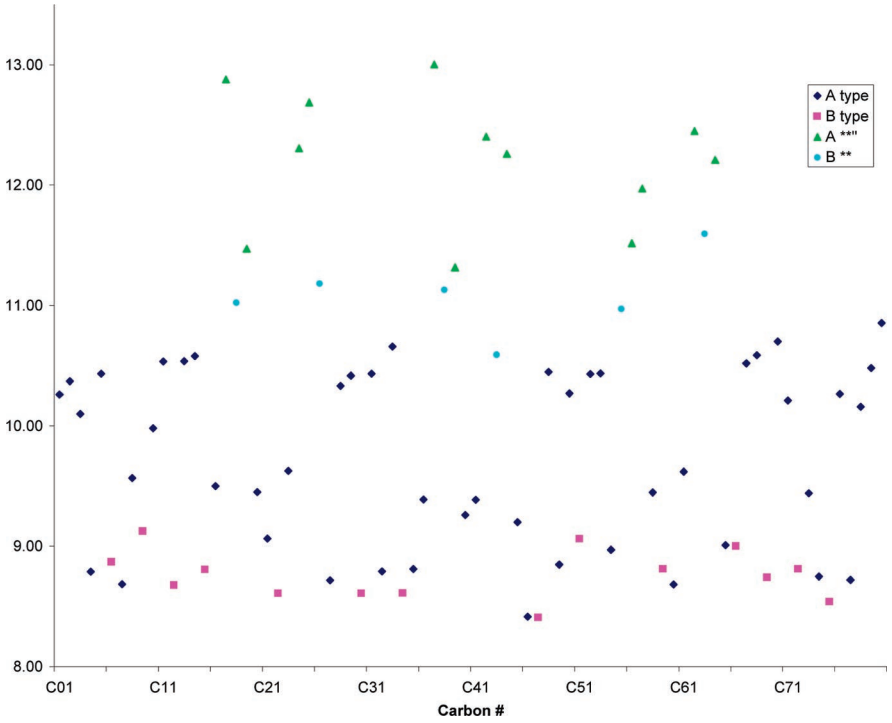

Figure 13. Pyramidalization angles, θ_p, for the fullerene carbon atoms in $(I_h)Tb_3N@C_{80}\cdot Ni^{II}(OEP)\cdot 2C_6H_6$.

largest group of structurally characterized TNT endohedrals. Of these five molecules, four (the I_h and D_{5h} isomers of $Tb_3N@C_{80}$, $Tb_3N@C_{86}$, and $Tb_3N@C_{88}$) have IPR structures, while only isomer 2 of $Tb_3N@C_{84}$ has a non-IPR structure.[16] Within this group it is clear that there is a correlation between the cage size and the structure of the Tb_3N group on the inside. For the three largest cages, isomer 2 of $Tb_3N@C_{84}$, $Tb_3N@C_{86}$, and $Tb_3N@C_{88}$, the Tb_3N units are planar, while for the two smallest, the I_h and D_{5h} isomers of $Tb_3N@C_{80}$, the Tb_3N units are significantly pyramidalized. In this context it is interesting to note that the Sc_3N unit retains its planar geometry through the entire series of related TNT endohedrals (the I_h and D_{5h} isomers of $Sc_3N@C_{80}$, $Sc_3N@C_{78}$, and $Sc_3N@C_{68}$) that have been crystallographically characterized. Of course, Sc(III) has a significantly smaller ionic radius than does Tb(III), and seems to readily fit in a planar fashion into all these cages including the smallest C_{68}. The small cage in $Sc_3N@C_{68}$ as the larger cages in $Tb_3N@C_{86}$, and $Tb_3N@C_{88}$ all have a flattened aspect that provides added space for the M_3N unit in the region perpendicular to the direction of flattening. Thus, the flattened shapes of these fullerenes appear especially effective in accommodating the internal M_3N groups and allowing them to assume planar geometries.

The pyramidalization of M_3N units within a C_{80} cage depends upon the size of the metal ions involved. Thus, small metal ions such as Sc(III) (ionic radius, 0.885 Å) and Lu(III) (ionic radius, 1.001 Å)[28] form TNT endohedrals with planar structures as found in the I_h and D_{5h} isomers of $Sc_3N@C_{80}$[29] and in $Lu_3N@C_{80}$.[29] Larger metal ions, such as Gd(III) (ionic radius, 1.078 Å) and Tb(III) (ionic radius, 1.063 Å),[28] exhibit pyramidal structures in the I_h and D_{5h} isomers of $Tb_3N@C_{80}$ and in the I_h isomer of $Gd_3N@C_{80}$.[30] A smaller degree of pyramidalization is seen for the Y_3N group in a functionalized derivative of (I_h)-$Y_3N@C_{80}$,[26] an observation which is consistent with the intermediate size of Y(III) (ionic radius, 1.040 Å).[28]

The cage size is also correlated with length of the Tb−N and nearest Tb−C distances. As the data in Table 1 show, as the cages get larger, the Tb−N and nearest Tb−C distances increase. Additionally, the lengthening of the Tb−N distances allows the Tb_3N units to adopt planar structures in the larger cages.

In the crystals used in this study, the cage shape appears to be correlated with the positioning of the internal Tb_3N group with regard to the adjacent $Ni^{II}(OEP)$ molecule. Thus in the nearly spherical molecules the Tb_3N groups lie in an orientation that is roughly perpendicular to the porphyrin plane with two of the terbium ions nearly equidistant from the nickel ion and near the plane of the porphyrin. This arrangement of the internal metal ions with regard to the porphyrin plane has also been seen in other TNT endohedrals including $ErSc_2N@C_{80}$,[31] $CeSc_2N@C_{80}$,[25] and $Gd_3N@C_{80}$.[30] In $Tb_3N@C_{86}\cdot Ni^{II}(OEP)\cdot 3C_6H_6$ where the flattened side of the fullerene is aligned with the planar surface of the porphyrin, the Tb_3N unit lies parallel to the porphyrin plane. In $Tb_3N@C_{88}\cdot Ni^{II}(OEP)\cdot 2.5C_6H_6$ the fullerene cage appears to be too large to lie with its flat side against the porphyrin. Consequently, the cage as well as Tb_3N, the unit within it, is canted with regard to the plane of the porphyrin.

It is interesting to note that both of the large fullerenes examined here, $Tb_3N@C_{88}$ and $Tb_3N@C_{86}$, employ cage structures that are chiral. These join $Sc_3N@C_{68}$, which has D_3 symmetry and a similar flattened shape, to form the only group of unfunctionalized fullerenes with chiral structures to be characterized crystallographically. In all cases, these endohedrals

(28) Shannon, R. D. *Acta Crystallogr., Sect. A* **1976**, *32*, 751.
(29) Stevenson, S.; Lee, H. M.; Olmstead, M. M.; Kozikowski, C.; Stevenson, P.; Balch, A. L. *Chem.−Eur. J.* **2002**, *8*, 4528.
(30) Stevenson, S.; Phillips, J. P.; Reid, J. E.; Olmstead, M. M.; Rath, S. P.; Balch, A. L. *Chem. Commun*. **2004**, 2814.
(31) Olmstead, M. M.; de Bettencourt-Dias, A.; Duchamp, J. C.; Stevenson, S.; Dorn, H. C.; Balch, A. L. *J. Am. Chem. Soc*. **2000**, *122*, 12220.

form cocrystals with Ni^{II}(OEP) that form in centrosymmetric space groups, and consequently each crystal is a racemate. The similar external shapes of these endohedral fullerenes allow each enantiomer to occupy a common site with a different orientation that is proscribed by crystallographic symmetry.

In conclusion, it appears that the IPR rule is still a useful guide for our expectations for the structures of higher endohedral fullerenes, but the non-IPR structure of isomer 2 of $Tb_3N@C_{84}$ reminds us that caution is needed in regard to our expectations. On a positive note, it is very encouraging to find that only a small number of cages with discrete geometries are found for these higher endohedrals, despite the fact that many IPR cage choices are available and an overwhelming variety of non-IPR structures could be utilized for these large endohedrals. Obtaining pure samples of the enantiomers of $Tb_3N@C_{88}$ and $Tb_3N@C_{86}$ presents a new challenge with these important new nanomaterials.

Experimental

Synthesis of $Tb_3N@C_{2n}$. Graphite rods (6.15 mm diameter by 152 mm length) were core-drilled and subsequently packed with a mixture of Tb_4O_7, graphite powder and Fe_xN with a weight ratio of 2.03:1.0:0.4, respectively. These rods were then vaporized in a Krätschmer−Huffman generator under a dynamic flow of He and N_2 (flow rate ratio of N_2/He = 3:100) with a total pressure of ca. 300 Torr before arc discharge to obtain soot containing $Tb_3N@C_{2n}$. The resulting soot was then extracted with refluxing toluene in a Soxhlet extractor for 20 h to obtain the soluble extract that was used for purification.

Synthesis of CPDE-MPR. To prepare CPDE-MPR, 25 g (30 mmol Cl) of Merrifield peptide resin was suspended in 600 mL of toluene in a 1 L flask. The mixture was cooled to −20 °C and held at that temperature using a dry ice and ethyl alcohol bath. A 60 mL portion of a sodium cyclopentadienide solution (2 M in tetrahedrafuran) was added dropwise to the stirred suspension. After the addition was complete, the suspension was stirred at −20 °C for 2 h. The suspension was collected by vacuum filtration on a Buchner funnel and washed with water until the filtrate was colorless. Then the filtration and washing were repeated using toluene. The sample of CPDE-MPR was dried under a N_2 flow in the hood and kept in a glove box. The product is a light-brown solid.[32]

Separation of $Tb_3N@C_{2n}$. The extract was applied to a glass column (22 mm diameter by 280 mm length) packed with approximately 20 g of cyclopentadiene-functionized Merrifield resin (CPDE-MPR) in toluene. Toluene was flushed through by gravity feed (about 20 mL/h). The eluent was further separated using a two-stage HPLC approach. First, the pentabromobenzyloxypropyl silica, 5PBB, column (4.6 mm by 250 mm, Alltech Associates) was employed with toluene as the mobile phase. The flow rate was 2.0 mL/min and the detection wavelength was 390 nm. The fractions Tb2, Tb5, and Tb6 from this 5PBB column were collected and further separated with a 2-(1-pyrenyl)-ethyl silica, 5PYE, column (10 mm by 250 mm, Nacalai Tesque) using toluene as a mobile phase (2.0 mL/minute) to obtain pure samples of $Tb_3N@C_{2n}$.

Crystal Growth for Terbium Endohedrals. Cocrystals of $Tb_3N@C_{2n}$ and Ni^{II}(OEP) were obtained by layering a brown color solution of ca. 0.5 mg of $Tb_3N@C_{2n}$ in 0.5 mL benzene over a red benzene solution of Ni^{II}(OEP) in a glass tube. Over a 14 day period, the two solutions diffused together and black crystals formed.

X-ray Crystallography and Data Collection. The crystals were removed from the glass tubes in which they were grown together with a small amount of mother liquor and immediately coated with a hydrocarbon oil on the microscope slide. Suitable crystals were mounted on glass fibers with silicone grease and placed in the cold dinitrogen stream of a Bruker ApexII diffractometer with graphite-monochromated Mo Kα radiation at 90(2) K. Crystal data are given in Table 2. The structures were solved by direct methods and refined using all data (based on F^2) using the software of SHELXTL 5.1. A semiempirical method utilizing equivalents was employed to correct for absorption.[33] Hydrogen atoms were located in a difference map, added geometrically, and refined with a riding model.

Acknowledgment. We thank the National Science Foundation [Grants CHE-0413857 (A.L.B.), CHE-0443850 (H.C.D.) and DMR-0507083 (H.C.D.)] and the National Institute of Health [Grant 1R01-CA119371-01 (H.C.D.)] for support.

Note Added in Proof

Poblet and co-workers (Campanera, J. M.; Bo, C.; Poblet, J. M. *Angew. Chem. Int. Ed.* **2005**, *44*, 7230−7233) have predicted (on the basis of electronic structure calculations on empty cage anions) that no IPR fullerene cages between C_{60} and C_{84} other than C_{60}, D_{3h}-C_{78}, D_{5h}-C_{80}, and I_h-C_{80} will be capable of encapsulating an $(M_3N)^{6+}$ unit. That prediction was borne out for isomer 2 of $Sc_3N@C_{84}$, which has a non-IPR structure. No predictions involving C_{86} or C_{88} were made at that time.

Supporting Information Available: The HPLC chromatograms, UV−vis, and MS spectra of the purified samples; X-ray crystallographic files in CIF format for $Tb_3N@C_{88}\cdot Ni^{II}(OEP)\cdot 2.5C_6H_6$, $Tb_3N@C_{86}\cdot Ni^{II}(OEP)\cdot 3C_6H_6$, $(D_{5h})Tb_3N@C_{80}\cdot Ni^{II}(OEP)\cdot 2C_6H_6$, and $(I_h)Tb_3N@C_{80}\cdot Ni^{II}(OEP)\cdot 2C_6H_6$. This material is available free of charge via the Internet at http://pubs.acs.org.

JA066437+

(32) Guhr, K. I.; Greaves, M. D.; Rotello, V. M. *J. Am. Chem. Soc.* **1994**, *116*, 5997.

(33) Sheldrick, G. M. *SADABS*, version 2.10; Bruker Analytical: Madison, WI, 2002 (based on a method of Blessing, R. H. *Acta Crystallogr., Sect. A.* **1995**, *51*, 33).